

A. Bevilacqua (1,2), C. Fourmentaux (2), A. Bertagnini (2), M. Bisson (2), T. Esposti Ongaro (2), F. Flandoli (3), R. Isaia (4), A. Neri (2), and M. Rosi (5)

(1) Scuola Normale Superiore, Pisa, Italy, (2) Istituto Nazionale di Geofisica e Vulcanologia, Sezione di Pisa, Pisa, Italy, (3) Università di Pisa, Dip.to di Matematica Applicata, Pisa, Italy, (4) Istituto Nazionale di Geofisica e Vulcanologia, Osservatorio Vesuviano, Napoli, Italy, (5) Università di Pisa, Dip.to di Scienze della Terra, Pisa, Italy

Geophysical Research Abstracts  
Vol. 14, EGU2012-6688, 2012  
EGU General Assembly 2012  
© Author(s) 2012

## Introduction

The Campi Flegrei (CF) (Fig 1) is an active volcanic area located in the Campanian Plain, along the Tyrrhenian margin of the Southern Apennines (Italy), dominated by the formation of a 12 km large, resurgent caldera. The nested Campi Flegrei caldera results from successive collapses related to the eruptions of the Campanian Ignimbrite (CI: 39.3±0.1 ka) and Neapolitan Yellow Tuffs (NYT: 14.9±0.4 ka). After the NYT eruption, volcanism was concentrated in three epochs of activity, alternating to periods of quiescence. The great majority of the eruptions have been explosive, variable in magnitude and also characterized by the generation of fallout, ash deposits and pyroclastic density currents (PDCs).

We present here a methodology aimed at the construction of a probability map of PDC hazard of the CF area. At this stage, results are preliminary and will be improved by future research work. Nevertheless, first outcomes already provide numerous insights in the problem and contribute to define future research directions.

In the study we had to cope with three different problems, related to different probability spaces:

- constructing a probability map of the place of a new vent opening
- giving a probability law to the area of invasion of a PDC from a fixed new vent
- choosing a probability distribution for the uncertainty that affects the model itself

To calculate the probabilistic simulations we used the R statistics software, and to plot the maps we used the ESRI platform.



Fig 1 - High resolution image of Campi Flegrei (Bisson et al., 2007)

## Drawing the zones

We have divided the CF area in 14 zones following a simple hierarchical way: starting with macroscopical divisions and ending with more detail, trying to isolate every single zone that has different geological characteristics (Fig 2). Subdivisions were articulated in four different levels starting from Level 0 to Level 3.

The freedom in the shapes of the zones permits an optimal representation of the geological and morphological differences that characterize each zone.

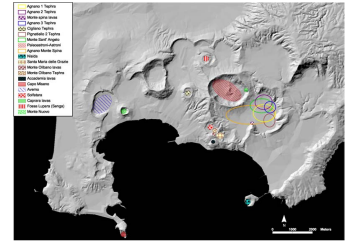


Fig 3 - Preliminary uncertainties affecting the vent locations of the events occurred in the last 5Kyr

## From the data to the weights

As a first step we focused on every single zone of the more detailed level (Level 3). We then defined a way to assign a precise amount of points to each of them, using as much as possible the information we have about it. In particular in this preliminary work we assigned points to the following volcanological features (see Tab 1):

Feature	Weight	Points	Percentage
Epoca I	1	100	10.0%
Epoca II	2	200	20.0%
Epoca III	3	300	30.0%
Epoca IV	4	400	40.0%
Epoca V	5	500	50.0%
Epoca VI	6	600	60.0%
Epoca VII	7	700	70.0%
Epoca VIII	8	800	80.0%
Epoca IX	9	900	90.0%
Epoca X	10	1000	100.0%

Feature	Weight	Points	Percentage
Epoca I	1	100	10.0%
Epoca II	2	200	20.0%
Epoca III	3	300	30.0%
Epoca IV	4	400	40.0%
Epoca V	5	500	50.0%
Epoca VI	6	600	60.0%
Epoca VII	7	700	70.0%
Epoca VIII	8	800	80.0%
Epoca IX	9	900	90.0%
Epoca X	10	1000	100.0%

Table 1 - Weights assignment to the zones of hierarchical Levels

## The probability map of new vents opening

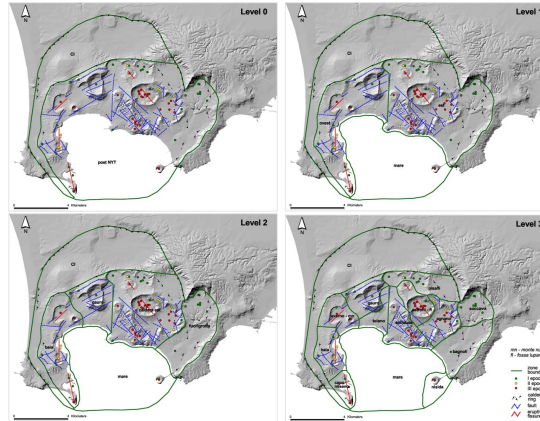


Fig 2 - Hierarchical Levels used in the subdivision of the CF caldera

To draw the lines of separation between different zones we used key volcanological information such as the vent locations, presence of faults and eruptive fissures, presence of crater rims and the occurrence of vent clusters. Main references for these features were the maps of Viarado et al. (2010) and Smith et al. (2011). In particular the different zones were drawn by considering the different uncertainties affecting the vent location of the events occurred in the last 5Kyr (Fig 3).

- the number of past vents as a function of their specific epoch
- the faults

Other features such as the possible presence of hidden vents, the occurrence of uplifting phenomena, gas emissions or seismic activity were not included at this stage although they could be considered in a future work or during a possible unrest.

In order to avoid to exclude any potential area of vent opening we also defined a "homogeneity coefficient" K, that allowed to assign new points to each zone proportionally to the relative area extension. Increasing or decreasing it we could get a more or less homogeneous map. Based on data analysis we assumed values of K in the range between 0.35 and 0.5.

At last, we normalized the points of each zone to obtain a first probability distribution (in percentage) on the 14 zones considered at the third level. By summing the values of the different zones we would then get the probabilities associated to the zones represented at the previous levels (Levels 0-2).

All the procedure is as flexible as possible and could be further improved to incorporate the many different features of the volcano.

## The expert elicitation adjustment

Based on the weights assigned to the different volcanological features we got a first probability map of vent opening. But we could try to further improve it including additional features of the volcanic system that were not considered. Examples are the magmatic signature of the products erupted in the different regions as well as the type of eruption occurred as a function of space.

Therefore, based on the expert opinions and starting from the Level 0 to Level 3 we could reassign the conditional probability of every division, using the coarse map as a guide (see Tab 2). After this expert elicitation it is possible to recalculate the weight of every single zone so obtaining an improved probabilistic vent opening map. This adjustment also permits a fast way to change the map in case of evolution of the volcanic system.

Level	Feature	Weight	Points	Percentage	
LEVEL 0	Epoca I	1	100	10.0%	
	Epoca II	2	200	20.0%	
	Epoca III	3	300	30.0%	
	Epoca IV	4	400	40.0%	
	Epoca V	5	500	50.0%	
	Epoca VI	6	600	60.0%	
	Epoca VII	7	700	70.0%	
	Epoca VIII	8	800	80.0%	
	Epoca IX	9	900	90.0%	
	Epoca X	10	1000	100.0%	
	LEVEL 1	Epoca I	1	100	10.0%
		Epoca II	2	200	20.0%
		Epoca III	3	300	30.0%
		Epoca IV	4	400	40.0%
Epoca V		5	500	50.0%	
Epoca VI		6	600	60.0%	
Epoca VII		7	700	70.0%	
Epoca VIII		8	800	80.0%	
Epoca IX		9	900	90.0%	
Epoca X		10	1000	100.0%	
LEVEL 2		Epoca I	1	100	10.0%
		Epoca II	2	200	20.0%
		Epoca III	3	300	30.0%
		Epoca IV	4	400	40.0%
	Epoca V	5	500	50.0%	
	Epoca VI	6	600	60.0%	
	Epoca VII	7	700	70.0%	
	Epoca VIII	8	800	80.0%	
	Epoca IX	9	900	90.0%	
	Epoca X	10	1000	100.0%	
	LEVEL 3	Epoca I	1	100	10.0%
		Epoca II	2	200	20.0%
		Epoca III	3	300	30.0%
		Epoca IV	4	400	40.0%
Epoca V		5	500	50.0%	
Epoca VI		6	600	60.0%	
Epoca VII		7	700	70.0%	
Epoca VIII		8	800	80.0%	
Epoca IX		9	900	90.0%	
Epoca X		10	1000	100.0%	

Table 2 - Expert elicitation proposed to improve the accuracy of probability values

## Plotting and smoothing

After the calculation of the densities of probability on every zone defined (Level 3) it was possible to plot coloured maps of the probability distribution of vent opening on the caldera. Maps could represent the distribution of probability in the 14 different zones by using different degrees of smoothing. In case of smoothing we choose to smooth the values of density within a fixed ray of distance. Different maps were produced using smoothing distances ranging between 500 and 1000 m (see Fig 4).

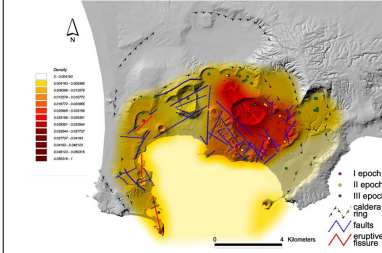


Fig 4 - Map of new vent opening, smoothing of 500 m

## Uncertainty quantification

An important objective of the methodology adopted is to quantify the uncertainty affecting the outcomes. Following the approach of Selva et al. (2011) we chose to define a Dirichlet distribution around the mean value represented by the calculated map (see Fig 5 - Tab 3). A key difference with respect to their work is that they have 700 different computational cells (and therefore Dirichlet functions) whereas we have just 14 zones to cope with.

In particular around the value of percentage of vent opening associated to every single zone we put a bell shaped probability distribution with a mean width of about 5%.

A future development will further investigate how to effectively incorporate the Bayesian approach into our model to have a better estimation of uncertainty.

Feature	Percentile 0%	Percentile 50%	Percentile 95%
Epoca I	0.00%	0.20%	4.11%
Epoca II	0.79%	4.01%	11.43%
Epoca III	0.19%	1.62%	7.39%
Epoca IV	0.21%	2.17%	8.69%
Epoca V	0.90%	17.40%	28.37%
Epoca VI	0.72%	17.28%	28.99%
Epoca VII	5.02%	15.21%	24.00%
Epoca VIII	0.03%	1.68%	6.20%
Epoca IX	1.45%	13.84%	13.84%
Epoca X	1.75%	6.12%	14.61%
Epoca XI	0.29%	2.54%	9.22%
Epoca XII	0.79%	3.96%	11.43%
Epoca XIII	2.25%	7.09%	16.00%

Table 3 - Percentiles associated to each zone

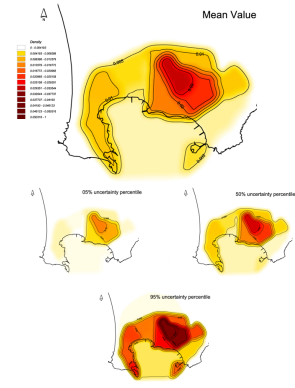


Fig 5 - Percentiles of uncertainty on the map, smoothing of 500 m

## The area of invasion of PDCs

A key step to produce meaningful probability maps of pyroclastic density current hazard is to quantify the area invaded by the flows given the location of the vent and the present topography of the volcano. This objective could be investigated by performing multidimensional and transient simulations of the flow dynamics (e.g. Esposti Ongaro et al., this EGU 2012 conference).

In this first application we adopted empirical estimators of the area invaded by pyroclastic density currents derived from field investigations. By using a maximum likelihood method we fitted a lognormal distribution to the areas of flow invasion as reconstructed by Orsi et al. (2004). In particular we derived two different estimators: one related to the events of the past 5k years, and the other related to the past 15k years (Fig 6a,b).

For simplicity, as a first guess, we assumed circular areas of invasion of the flows, therefore neglecting the present topographic features of the caldera.

## The Monte Carlo algorithm to produce hazard maps

In order to produce the probabilistic hazard map we subdivided the CF area in a grid of cells of 500m as side, assigning to each cell the value of probability associated to that area by the map of vent opening. We chose to represent the hazard of invasion by extracting randomly the extension of an area and spreading it circularly from every cell by using the same weight of the cell. We repeated this procedure 500 times and we took the mean to obtain a map of hazard. In this way, in every cell, we computed the mean probability to be reached by a PDC.

To produce maps representing the probability of flow invasion generated by events smaller than a fixed size, we truncated the lognormal invasion law to the chosen percentile and repeated the same algorithm.

## Comparing the maps of PDC hazard from different new vent opening maps

Starting from our new map (Fig 4), then starting also from the map by Selva et al. (2011), and restricting the probability to the cells ashore, we used the simple algorithm above to calculate different PDC hazard maps (Fig 7, Fig 8a).

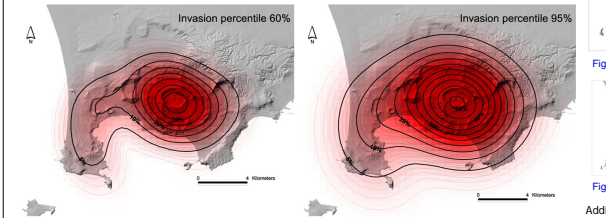


Fig 7 - Preliminary PDC hazard maps for two different runout exceedence probabilities (60% and 95%)

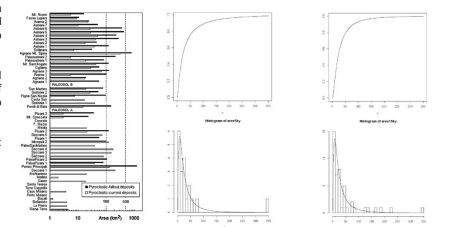


Fig 6 - a) Areas of PDCs invasion (Orsi et al., 2004) b) The lognormal distributions

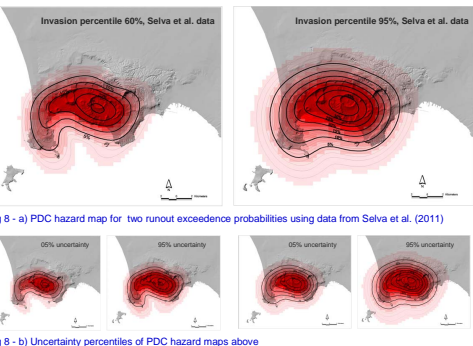


Fig 8 - a) PDC hazard maps for two runout exceedence probabilities using data from Selva et al. (2011) b) Uncertainty percentiles of PDC hazard maps above

Additionally, from the maps by Selva et al. (2011) we got the 05% and 95% percentile maps of this model of the PDC hazard also with respect to the Dirichlet distribution of the uncertainty of their map of new vent opening (Fig 8b).

## Concluding remarks

The adopted methodology allowed to obtain new probabilistic maps of vent opening and first maps of pyroclastic density current invasion at CF.

The new vent opening map allows to consider directly some of the uncertainties affecting the system such as that on vent location.

The preliminary hazard map of PDC invasion allows to consider first-order effect of the variability of vent opening on the areas at risk.

Estimates of invasion areas were only based on the reconstruction of past events and therefore consider an average effect of the caldera topography on the flow propagation.

Future improvements should implement more accurate description of the areas invaded based on the present topography of the caldera (e.g. 3D modelling of the PDC dynamics) as well as a more accurate assessment of the uncertainties involved.

**Acknowledgment:** this work was partially supported by the Dipartimento della Protezione Civile e Regione Campania, Italia.

**References:** Bevilacqua A., Bertagnini A., Mazzoni F. (2007) SITOEGO: A geographic database used for GIS applications. Il Nuovo Cimento C - Note Brevi - DOI 10.1394/nc/2007\_10243-9, 30C, N.3

Esposti Ongaro T., Neri A., Todisco M., Assessing pyroclastic density current dynamics and hazard of Plinian events at Campi Flegrei (Italy) by using 3D numerical simulations. EGU General Assembly 2012

Orsi G., Di Vito M. A., Isaia R. (2004) Volcanic hazard assessment at the restless Campi Flegrei caldera. Bull. Volcanol 66:514-530 DOI 10.1007/s00445-003-0338-4

Selva J., Orsi G., Di Vito M. A., Mercoletti W., Sardi L. (2011) Probability hazard map for future vent opening at the Campi Flegrei caldera, Italy. Bull. Volcanol. DOI 10.1007/s00445-011-0528-2

Smith V. C., Isaia R., Pearce N.J.G. (2011) Topostratigraphy and glass compositions of post-15 kyr Campi Flegrei eruptions: implications for eruption history and chronostratigraphic markers. Quaternary Science Reviews 30: 3638-3660

Viarado G., Isaia R., Ventura G., De Martino P., Terranova C. (2010) InSAR Permanent Scatterer analysis reveals fault re-activation during inflation and deflation episodes at Campi Flegrei caldera. Remote Sensing of Environment 114: 2373-2383